



Universidad Autónoma  
de Madrid

**Biblos-e Archivo**  
Repositorio Institucional UAM

Repositorio Institucional de la Universidad Autónoma de Madrid

<https://repositorio.uam.es>

Esta es la **versión de autor** del artículo publicado en:

This is an **author produced version** of a paper published in:

Molecular Genetics and Metabolism 125.3 (2018): 266-275

**DOI:** <https://doi.org/10.1016/j.ymgme.2018.09.008>

**Copyright:** © 2018 Elsevier Inc.. This manuscript version is made available under the CC-BY-NC-ND 4.0 licence <http://creativecommons.org/licenses/by-nc-nd/4.0/>

El acceso a la versión del editor puede requerir la suscripción del recurso

Access to the published version may require subscription

**Identification of 34 novel mutations in propionic acidemia: functional characterization of missense variants and phenotype associations.**

Ana Rivera-Barahona<sup>1,2,3,4</sup>, Rosa Navarrete<sup>1,2,3,4</sup>, Raquel García-Rodríguez<sup>1,2,3,4</sup>, Eva Richard<sup>1,2,3,4</sup>, Magdalena Ugarte<sup>2,3,4</sup>, Celia Pérez-Cerda<sup>2,3,4</sup>, Belén Pérez<sup>1,2,3,4</sup>, Alejandra Gámez<sup>1,2,3,4</sup>, Lourdes R Desviat<sup>1,2,3,4</sup>

<sup>1</sup>Centro de Biología Molecular Severo Ochoa UAM-CSIC, Universidad Autónoma, Madrid, Spain

<sup>2</sup>Centro de Diagnóstico de Enfermedades Moleculares (CEDEM), Madrid, Spain

<sup>3</sup>Centro de Investigación Biomédica en Red de Enfermedades Raras (CIBERER), ISCIII

<sup>4</sup>Instituto de Investigación Sanitaria Hospital La Paz (IdiPaz), ISCIII

*Correspondence to:*

Lourdes R. Desviat

Centro de Biología Molecular Severo Ochoa

Universidad Autónoma de Madrid

28049 Madrid, Spain

Phone: 34-911964566

Fax: 34-911964420

Email: [lruiz@cbm.csic.es](mailto:lruiz@cbm.csic.es)

## Abstract

Propionic acidemia (PA) is caused by mutations in the *PCCA* and *PCCB* genes, encoding  $\alpha$  and  $\beta$  subunits, respectively, of the mitochondrial enzyme propionyl-CoA carboxylase (PCC). Up to date, more than 200 pathogenic mutations have been identified, mostly missense defects. Genetic analysis in PA patients referred to the laboratory for the past 15 years identified 20 novel variants in the *PCCA* gene and 14 in the *PCCB* gene. 21 missense variants were predicted as probably disease-causing by different bioinformatics algorithms. Structural analysis in the available 3D model of the PCC enzyme indicated potential instability for most of them. Functional analysis in a eukaryotic system confirmed the pathogenic effect for the missense variants and for one amino acid deletion, as they all exhibited reduced or null PCC activity and protein levels compared to wild-type constructs. *PCCB* variants p.E168del, p.Q58P and p.I460T resulted in medium-high protein levels and no activity. Variants p.R230C and p.C712S in *PCCA*, and p.G188A, p.R272W and p.H534R in *PCCB* retained both partial PCC activity and medium-high protein levels. Available patients-derived fibroblasts carriers of some of these mutations were grown at 28°C or 37°C and a slight increase in PCC activity or protein could be detected in some cases at the folding-permissive conditions. Examination of available clinical data showed correlation of the results of the functional analysis with disease severity for most mutations, with some notable exceptions, confirming the notion that the final phenotypic outcome in PA is not easily predicted.

**Keywords:** propionic acidemia; *PCCA*; *PCCB*; novel mutations; structural analysis; folding; genotype-phenotype

## 1. Introduction

Propionic acidemia (PA, MIM#606054, ORPHA:35) is one of the most frequent life-threatening organic acidemias, caused by a deficiency of the mitochondrial propionyl-CoA carboxylase (PCC) enzyme, that catalyzes the carboxylation of propionyl-CoA to D-methylmalonyl-CoA, which eventually enters the Krebs cycle as succinyl-CoA [1]. Propionyl-CoA is common to the pathway for degradation of some amino acids (isoleucine, valine, threonine and methionine), odd-chain fatty acids, and cholesterol. Gut bacteria fermentation is also a source of propionyl-CoA. Most patients have a neonatal presentation with ketoacidosis, feeding refusal, lethargy, failure to thrive, seizures and encephalopathy, but there are also milder late-onset forms [2]. Advances in supportive treatment based on dietary restriction in order to restrict propiogenic substrates, carnitine supplementation to remove propionyl-CoA groups by enhancing urinary excretion and prevention of carnitine deficiency, and metronidazole to reduce propionate production from flora bowel, have allowed patients to live beyond the neonatal period. However, natural progression of PA leads to intellectual deficits, and increased risk for potentially lethal multiorgan complications, such as cardiomyopathies and pancreatitis, even for patients under good metabolic control [3-5].

Biochemically, this disorder is characterized by accumulation of propionyl-CoA, considered as the major toxic agent, and metabolites of alternative propionate oxidation. Several studies support the hypothesis that secondary mitochondrial dysfunction induced by accumulating propionyl-CoA and other toxic metabolites plays a major role in the pathomechanisms of PA. The evidence underlying this conclusion has been obtained from studies on patient biopsies, animal models or patients-derived fibroblasts [3, 6-10].

At the molecular level, PA is caused by mutations in either the *PCCA* or *PCCB* genes encoding both subunits,  $\alpha$  and  $\beta$ , respectively, of the PCC enzyme. To date, 124 variants in the *PCCA* gene and 112 in the *PCCB* gene are collected in the Human Genome Mutation Database (HGMD® Professional 2018.1). A review listing published variants in both genes was recently published [11]. *PCCA* gene is located in chromosome 13q32.3 and comprises 24 exons. *PCCB* gene is located in chromosome 3q22.3 and comprises 15 exons. In both genes, missense mutations are predominant (~50%), followed by small insertions/deletions and



splicing mutations and, in the case of the *PCCA* gene, by large genomic deletions (18%) associated to the presence of intronic repetitive elements [12]. Most patients are compound heterozygotes, hindering the establishment of genotype-phenotype correlations, although there are specific associations of certain missense mutations with mild phenotypes or of functionally “null” mutations with the most severe phenotypes [13, 14].

The native PCC enzyme is a dodecamer in a  $\alpha_6\beta_6$  configuration, with the  $\alpha$ -subunits arranged as monomers decorating a central  $\beta_6$  hexamer [15]. The  $\alpha$ -subunit has biotin carboxylase (BC), biotin-carboxyl carrier protein (BCCP) and biotin transfer (BT) domains, while the  $\beta$  subunit has a carboxytransferase (CT) domain. The BC, BCCP and CT domains are common structural features in acyl-CoA carboxylases [16], while the BT domain is unique to PCC and plays a key role in the interactions between the  $\alpha$  and  $\beta$  subunits [15]. The PCC crystal structure has provided a framework for elucidating the structural basis of PA-causing missense mutations [9, 15].

To date, PA is included in newborn screening programs in many developed countries [17, 18]. Affected individuals show elevated C3 (propionylcarnitine) and second tier biochemical testing guides the diagnosis, which is confirmed by detection of biallelic pathogenic variants in *PCCA* or *PCCB* or of deficient PCC enzymatic activity. Genetic diagnosis is fundamental for carrier testing in at-risk relatives and for precise prenatal diagnosis in affected families [2]. However, genetic heterogeneity is high, and novel variants of unknown clinical significance (missense mutations or small in-frame deletions) are frequently identified. Usually, a combination of *in silico* tools, focused on protein structural features and amino acids conservation, are used to distinguish potentially pathogenic variants [19]. Even so, functional assays are mandatory to interpret accurately the effect of sequence variation, which is critical for correct genetic diagnosis and for understanding the phenotypic expression of the disease. In this work, we report 20 novel mutations in the *PCCA* gene and 14 in the *PCCB* gene and provide expression data and structural analysis for the missense mutations, as a basis to understand the associated phenotypic characteristics.

## 2. Materials and methods

### 2.1 Patients' samples and genetic analysis

Fibroblasts or whole blood samples from 30 patients diagnosed with PA based on clinical and/or biochemical data were referred to the laboratory for genetic analysis. The study includes novel *PCCA* and *PCCB* variants identified in patients referred between 06/2003 to 04/2017, diagnosed either by selective metabolic screening or after newborn screening (NBS). Genetic analysis was performed by Sanger sequencing of both the *PCCA* and *PCCB* genes or by Massive Parallel Sequencing (MPS). This was performed using either a targeted customized exome sequencing panel to capture the exome of 120 genes involved in metabolic disorders (Nextera Nature Capture, Illumina, San Diego, California, USA) or an extended panel (Clinical-Exome Sequencing TruSight™ One Gene Panel, Illumina) that includes all the known (in 2013) disease-associated genes described in the OMIM database. Potentially pathogenic variants identified by MPS were confirmed by Sanger sequencing. When parental samples were available, biallelic inheritance was confirmed by Sanger sequencing. Deletion analysis in the *PCCA* gene was performed using Multiplex Ligation-dependent Probe Analysis (SALSA P278 PCCA MLPA kit, MRC-Holland). Ethical approval for the present study was granted by the Institutional Ethics Committee (Universidad Autónoma de Madrid).

*PCCA* and *PCCB* deficient fibroblast cell lines stably transformed with the T22 plasmid which contains SV40 DNA sequences [20, 21] were used for *in vitro* expression analysis. Control (CC2509, Lonza Inc., Allendale, NJ, USA) and patients-derived fibroblasts (P8, P18 and P22, Table 1) between passages 5 and 15 were grown at 37°C or under permissive folding conditions (28°C) to examine the potential effect of missense variants on protein stability. Cells were cultivated according to standard procedures. Briefly, cells were maintained in Minimum Essential Medium supplemented with 1% glutamine, 5-10% foetal bovine serum (FBS) and antibiotics.

### 2.2 *In silico* and *in vitro* functional analysis

To investigate the potential functional effect of the novel missense mutations, different bioinformatic algorithms were used: MutPred

(<http://mutpred.mutdb.org/>), Mutation Taster (<http://www.mutationtaster.org/>), Polyphen-2 (<http://genetics.bwh.harvard.edu/pph2/>) and SIFT (<http://sift.jcvi.org/>). Variants detected by MPS were analysed using Alamut Visual software, which combines the last three predictors.

For in vitro analysis, *PCCA* and *PCCB* deficient established fibroblast cell lines [20, 21] were used. *PCCA* and *PCCB* mutations were introduced by PCR mutagenesis (Quikchange Lightning Site-Directed Mutagenesis kit, Agilent Technologies, Santa Clara, CA) in the pCMVA45-12 and pRcCMVB52 vectors coding for wild-type *PCCA* and *PCCB* cDNAs, respectively. Sequence analysis confirmed the identity of the mutant clones and revealed that no other mutation was present in the full-length cDNA. The day before transfection, cells were seeded into 6-well culture cell plates (400,000 cells per well). Transfection was achieved by lipofection using Lipofectamine 2000 (Invitrogen), co-transfecting 2 µg of the mutant *PCCA* or *PCCB* vectors and 2 µg of the wild-type partner *PCCB* or *PCCA* constructs to achieve maximal expression [20]. Cells were harvested 72 h after transfection.

### 2.3 PCC enzymatic assay

PCC activity was assayed by measuring the enzyme-dependent incorporation of [14C]-bicarbonate into non-volatile products from the Krebs cycle as previously described [22]. Briefly, cells were resuspended in 20 mM Tris-HCl pH 8.0 buffer with 0.81 mM glutathione and excised by freeze-thaw cycles. The enzymatic reaction was initiated with the addition of the homogenate, maintained at 30°C during 20 min and stopped with trichloroacetic acid (TCA 30%). The samples were centrifuged during 15 min at 16,873 x g, the supernatant transferred to a scintillation vial and subjected to an evaporation process at room temperature for 24-48 hours. The non-volatile products were measured in a 1209 Rackbeta Liquid Scintillation Counter (Wallac) after 24 hours. PCC activity is expressed in pmols of incorporated [14C] min<sup>-1</sup> mg<sup>-1</sup> of total protein. Protein concentration in cellular extracts was determined by the Bradford method (Bio-Rad Laboratories, Hercules, CA, USA).

### 2.3 Western blot

Cells were disrupted by freeze-thawing in lysis buffer (10 mM Tris-HCl pH 7.5, 150 mM NaCl, 0.1% triton X-100 and 10% glycerol) with protease inhibitors and centrifuged 30 min at 4°C. The supernatant fraction was collected and protein concentration was determined by the Bradford method (Bio-Rad Laboratories, Hercules, CA, USA). Equal amounts of lysed extracts (50 µg protein) were loaded on a 10% SDS-polyacrylamide gel. After electrophoresis, proteins were transferred to a nitrocellulose membrane (iBlot Gel Transfer Stacks, Regular) in an iBlot Gel transfer device (Invitrogen, Carlsbad, CA, USA). Immunodetection was carried out using commercially available antibodies against PCCA (1:500, Santa Cruz Biotechnology, Santa Cruz, CA, USA) or PCCB (1:500, Santa Cruz Biotechnology, Santa Cruz, CA, USA). Secondary antibody used was goat anti-mouse (1:5,000, Santa Cruz Biotechnology, Santa Cruz, CA, USA). For loading control, membranes were immunostained with GAPDH antibody (1:5,000, Abcam, Cambridge, UK). Antibody binding was detected by enhanced chemiluminescence (GE Healthcare, Buckinghamshire, UK). Protein quantification was performed using a calibrated densitometer GS-900 (Bio-Rad Laboratories, Hercules, CA, USA).

### 2.4 Structural analysis

PCC holoenzyme is a trimer of hetero-tetramers composed by two central  $\beta$ -subunits and two peripheral  $\alpha$ -subunits. Structural analysis of *PCCA* and *PCCB* mutations was performed in a homology model using as template the homologous crystallized PCC holoenzyme from *Ruegeria pomeroyi* (PDB ID: 3n6r) [15], composed of  $\alpha$  and  $\beta$ -subunits sharing 54% and 65% sequence identity to the human subunits, respectively. The  $\alpha$ -subunit has been modelled from an analogous  $\alpha$ -subunit of *S. aureus* bound to an ATP analogue (AMPPNP) (PDB ID: 2vpq) [23]. Homology modelling was performed as previously described [9].

### 3. RESULTS

#### 3.1 Mutation identification

The molecular and available clinical data of the patients included in the study are shown in Table 1. A total of 34 novel allelic variants, 20 in the *PCCA* gene and 14 in the *PCCB* gene, were identified in 30 patients diagnosed with PA (Figure 1). All variants, with the sole exception of *PCCA* p.L470R, are private, present in only one family. None of the variants are present in public databases (HGMD professional release 2018.1, ClinVar) and have a minor allele frequency (MAF) of less than 1% in the ExAC server. In the *PCCA* gene, we identified 11 single-nucleotide changes predicted to result in missense variants (Table 2), three to affect the splicing process (c.101\_105+5delinsGCAACGGG, c.600+1G>A and c.1540+1G>C), one nonsense change (c.1218C>G; p.Y406\*) and five out-of-frame small deletions (c.443del, c.503\_506del, c.1364\_1365del, c.1477del, c.1495del) (Figure 1).

RT-PCR analysis in patients' fibroblasts carrying the c.600+1G>A and c.1540+1G>C mutations showed exon skipping (exon 7 and 17, respectively) (data not shown). The c.101\_105+5delinsGCAACGGG mutation abolishes the 5' splice site of exon 1. cDNA analysis was only possible for 3' end fragments, the 5' end region could not be amplified.

In the *PCCB* gene we identified 10 missense variants and one amino acid deletion (Table 2), two out-of-frame deletions (c.1172\_1173del and c.1314del) and one splicing change abolishing the conserved 3' splice site of exon 14 (c.1399-2\_-1del) (Figure 1). For the splicing mutation, no cDNA analysis could be performed as only genomic DNA was available.

The potential pathogenic effect of missense and in-frame mutations in the *PCCA* and *PCCB* genes was investigated *in silico* using different bioinformatic prediction softwares (Table 2). All the changes are clearly predicted as possibly pathogenic, with the exception of p.C712S (*PCCA* gene) and p.G356R (*PCCB* gene), which scored as neutral changes using PolyPhen-2 but as damaging or disease-causing according to the other software.

### 3.2 Functional analysis of *PCCA* and *PCCB* variants

The predicted missense changes and one amino acid deletion (p.E168del) were analysed using an established eukaryotic expression system to confirm their pathogenicity. The mutant *PCCA* or *PCCB* constructs were expressed in *PCCA* and *PCCB* deficient fibroblast cell lines, respectively, according to established procedures [20, 21] and the resulting PCC activity and *PCCA* or *PCCB* proteins were quantified. The results are shown in Figure 2. *PCCA* variants p.C712S and p.R230C retained some residual activity (7-8%), corresponding to *PCCA* protein levels of 2.4 and 25%, respectively, while the rest exhibited null or very low PCC activity and *PCCA* protein levels relative to the wild-type construct (Figure 2A). *PCCB* variants could be grouped in variants with null or very low PCC activity and protein (p.M316R, p.D382E, p.H250Y, p.G356R, p.R512H), variants resulting in medium-high protein levels and no activity (p.E168del, p.Q58P and I460T) and variants retaining partial activity and protein levels (p.R272W, p.H534R and p.G188A) (Figure 2B).

### 3.3 Structural analysis of *PCCA* and *PCCB* variants

The structural effect of the variants was carried out using a homology model of the human PCC holoenzyme [9]. The  $\alpha\beta\beta\alpha$  heterotetramer model was visualized with Pymol and missense PCC mutations were *in silico* mapped (Figures 3 and 4). In our study, most of the variants were predicted to disturb and destabilize protein structure (Tables 2 and 3). *PCCA* variants p.G175D and p.R399W predictably distort PCC active site by disrupting ATP,  $Mg^{++}$  and  $Cl^-$  binding (Figure 3D and 3G). *PCCA* and *PCCB* variants with undetectable PCC activity are predicted to cause large structural changes due to steric and folding hindrances between residues, changes in amino acid size or charge or disruption of  $\alpha$ -helices (Figures 3 and 4 and Table 3). Three *PCCB* variants were predicted to result in no substantial structural change: p.Q58P affects a  $\alpha$ -helix at the beginning of the polypeptide chain; p.G188A is located in a flexible region and p.H534R results in loss of interactions with nearby residues while allowing for new compensating ones (Figure 4A, 4C and 4K and Table 3).

### 3.4 Analysis in patients' fibroblasts grown at different temperatures

Control and available patients-derived fibroblasts (P8, P18 and P22, Table 1), heterozygous carriers of mutations p.R230C (*PCCA*), p.C712S (*PCCA*) and p.H205Y (*PCCB*), respectively, were grown at 37°C and at 28°C, in order to investigate the possibility of recovering PCC activity and protein at the folding permissive conditions. PCC activity was barely detectable for the 3 samples grown at 37°C, corresponding to 0.7-1.3% of the levels in control fibroblasts (mean 563.5±96.0 pmol/min/mg). At 28°C, PCC activity slightly increased for P8 and P18. Western blot analysis showed a positive stabilization effect of the permissive temperature for mutant *PCCA* or *PCCB* protein present in P8 and P22, respectively (Figure 5).

## 4. Discussion

Genotyping analysis using standard or massive parallel sequencing approaches led to the identification of novel candidate variants in the *PCCA* or *PCCB* genes in patients with a biochemical/enzymatic diagnosis of PA. Correct assignment of pathogenicity is of utmost importance for correct prognosis and genetic counselling, as well as to avoid false annotations of causality at the variants level in public databases. Twelve of the novel variants have a clear damaging effect on gene function and are thus assumed to be disease-causing. They include 4 splicing defects (3 in *PCCA*, shown to result in aberrant splicing in patients' cells, and 1 in *PCCB*), one nonsense variant in the *PCCA* gene and 7 out-of-frame small deletions (5 *PCCA* and 2 *PCCB*).

The remaining variants correspond to missense changes and to one amino acid deletion, which *in silico* are predicted to be damaging or disease-causing (Table 2). In this work, we have experimentally validated these predictions, assessing protein levels (as a measure of protein stability) and enzymatic activity using an established eukaryotic expression system. To complement the *in vitro* studies, the structural environment of the affected residues and the predicted alterations resulting from the variant changes have been analysed in a 3D model of the enzyme. Most of the *PCCA* missense variants map along the BC domain, with just one (p.C712S) located in the BCCP domain. In *PCCB*, the variants are

spread along the protein. Only *PCCA* variants p.G175D and p.R399W directly affect the active site, correlating with the lack of enzymatic activity. The remaining variants affect residues with no catalytic roles, arguing in favour of an effect on stability of the resulting mutant proteins. Structural predictions for *PCCB* variants p.Q58P, p.G188A and p.H534R indicate no substantial effect on protein structure, correlating with medium-high residual protein levels.

Based on the overall results, we suggest a possible classification of the analysed mutations as follows: (1) destabilizing mutations that retain some protein and residual activity, (2) catalytic mutations that affect enzymatic activity and (3) destabilizing mutations resulting in null or very low residual activity (Table 2). Most *PCCA* variants are classified as group 3, except for p.R230C and p.C712S which retain some protein and activity (group 1) and p.G175D and p.R399W that directly affect the active site (group 2). Regarding *PCCB* variants, p.G188A, p.R272W and p.H534R are classified as group 1 and p.H250Y, p.M316R, p.G356R, p.D382E and p.R512H as group 3. Variants p.Q58P, p.E168del and p.I460T exhibit mixed properties of groups 1 and 2, as they retain medium-high protein levels but are completely devoid of activity. Degradation bands of the three mutant proteins are detected by western blotting (Figure 2B), consistent with a folding, degradation-prone defect. Obviously, the catalytic and stability properties of the mutant proteins are interdependent and together contribute to the final functional outcome.

Our results agree with previous studies indicating that the loss of function of most PCC mutant proteins is based on protein reduction due to decreased stability [24-26], probably related to a higher susceptibility to degradation or aggregation compared with the wild-type protein, a common mechanism underlying many monogenic diseases [27-30]. The degradation of PCC proteins harbouring missense mutations might be promoted by a folding defect or lie in a problem of hetero-oligomeric assembly [24, 26]. The results from the expression of patients' fibroblasts at 28°C provide additional evidence of a folding defect for certain missense mutations. We could detect slight increases in PCC activity or protein at the folding-permissive temperature, suggesting that the administration of compounds that improve PCC folding might provide a treatment for a large number of patients who could benefit from such folding therapy. The use of small



therapeutic molecules, such as proteostasis regulators and/or pharmacological chaperones, has been proved to be viable therapeutic options for a range of genetic diseases caused by folding defects [30].

The clinical application of our study is the confirmation of the genetic diagnosis in patients, enabling accurate genetic counselling and, in many cases, providing a prognostic view of the probable course of the disease. However, the genetic heterogeneity present in PA patients, with most mutations being “private”, present in only one family, along with the practical absence of homozygosity among the studied patients, hinders a straightforward genotype–phenotype correlation. After the analysis of the available data, we observe that homozygous or functionally hemizygous patients with mutations predicted as severe (splicing, frameshift and missense mutations classified as group 3) had a neonatal presentation and present a severe phenotype (Tables 1 and 2). Patient P8 carries a mild folding *PCCA* mutation (p.R230C) correlating with a late presentation of the disease (at 2 years of age). Similarly, P21 is homozygous for *PCCB* mutation p.G188A that retains high residual activity *in vitro* correlating with late presentation and a mild phenotype. This mutation mimics the results obtained for the previously characterized variant p.N536D, exhibiting 80% activity *in vitro* and present in several patients with a mild clinical phenotype [21].

Some inconsistencies were also found in our series. There is no correlation between the mild clinical phenotype exhibited by P19 and the genotype, consisting of the severe catalytic mutation p.Q58P devoid of activity, in combination with a null mutation in the *PCCB* gene. Clearly, other genetic and external factors contribute to the final phenotypic presentation of the disease. On the other hand, P30, with a severe neonatal presentation, carries a mild missense mutation (p.H534R) with partial activity, in combination with a null mutation in the *PCCB* gene. To date, evidence has accumulated indicating that predicted missense mutations are in fact splicing mutations affecting regulatory sequences that contribute to exon definition [31]. This possibility was examined for c.1601A>G, predicted p.H534R, using Human Splice Finder (<http://www.umd.be/HSF3/>). No significant differences in predicted splice scores or splicing regulatory motifs were identified, indicating the variant has probably no impact on splicing. In any case, we must bear in mind that although the

eukaryotic system employed here is useful for initial functional characterization of the identified missense variants, the overexpression of the mutant proteins does not represent the exact cellular scenario in which the *PCCA* and *PCCB* proteins assemble to result in a functional oligomer. Therefore, caution must be exerted when predicting the clinical course in a patient, especially for private mutations.

In summary, this work represents a large-scale update on pathogenic mutations in the *PCCA* and *PCCB* genes causing PA, and confirms previous reports indicating a major causative role of mutation-induced protein destabilization, which is a common mechanism in many metabolic diseases [27, 32, 33]. This finding supports the idea that PA could be amenable to chaperone therapy to rescue folding defects.

## Acknowledgements

We thank the following physicians/clinicians for sending samples for genetic analysis: Dr Wilson (Auckland, New Zealand), Dr Parini (Rome, Italy), Dr Vilaseca (Barcelona, Spain), Dr Gockay (Istanbul, Turkey), Dr Al Sannaa (Saudi Arabia), Dr Pedrón (Madrid, Spain), Dr Savvapoulou (Thessalonica, Greece), Dr Martínez-Pardo (Madrid, Spain), Dr Lama (Madrid, Spain), Dr Lemes (Montevideo, Uruguay), Dr Van Calcar (Madison, USA), Dr Pintos (Badalona, Spain), Dr Laszlo (Szeged, Hungary), Dr Kuijtmans (Nijmegen, The Netherlands), Dr Schatz (München, Germany), Dr EL Khateeb (Jordan), Dr de las Heras (Baracaldo, Spain), Dr Miñana (Buenos Aires, Argentina). The technical assistance of A. Sánchez is gratefully acknowledged. This work was supported by Spanish Ministry of Economy and Competitiveness and European Regional Development Fund (grant number SAF2016-76004-R). Centro de Biología Molecular Severo Ochoa receives an institutional grant from Fundación Ramón Areces.

## References

- [1] W.A. Fenton, R.A. Gravel, L.E. Rosenberg, Disorders of propionate and methylmalonate metabolism, in: C.R. Scriver, A.L. Beaudet, W. Sly, D. Valle (Eds.), *The Metabolic and Molecular Bases of Inherited Disease*, McGraw-Hill, New York, 2001, pp. 2165-2190.
- [2] O.A. Shchelochkov, N. Carrillo, C. Venditti, Propionic Acidemia, in: R.A. Pagon, M.P. Adam, H.H. Ardinger, S.E. Wallace, A. Amemiya, L.J.H. Bean, T.D. Bird, N. Ledbetter, H.C. Mefford, R.J.H. Smith, K. Stephens (Eds.), *GeneReviews(R)*, Seattle (WA), 1993.
- [3] E. Richard, B. Perez, C. Perez-Cerda, L.R. Desviat, Understanding molecular mechanisms in propionic acidemia and investigated therapeutic strategies *Expert Opinion on Orphan Drugs* 3 (2015) 1427-1438.
- [4] L. Pena, J. Franks, K.A. Chapman, A. Gropman, N. Ah Mew, A. Chakrapani, E. Island, E. MacLeod, D. Matern, B. Smith, K. Stagni, V.R. Sutton, K. Ueda, T. Urv, C. Venditti, G.M. Enns, M.L. Summar, Natural history of propionic acidemia *Mol Genet Metab* 105 (2012) 5-9.
- [5] L. Pena, B.K. Burton, Survey of health status and complications among propionic acidemia patients *Am J Med Genet A* 158A (2012) 1641-1646.
- [6] E. Richard, P. Rodriguez-Pombo, L.R. Desviat, B. Perez, B. Merinero, C. Perez-Cerda, M. Ugarte, Mitochondrial organic acidurias. Part II: Mitochondrial dysfunction, in: F. Palau, S. Cadenas (Eds.), *Mitochondrial Pathophysiology*, Research Signpost, Kerala (India), 2011, pp. 173-191.
- [7] M.A. Schwab, S.W. Sauer, J.G. Okun, L.G. Nijtmans, R.J. Rodenburg, L.P. van den Heuvel, S. Drose, U. Brandt, G.F. Hoffmann, H. Ter Laak, S. Kolker, J.A. Smeitink, Secondary mitochondrial dysfunction in propionic aciduria: a pathogenic role for endogenous mitochondrial toxins *Biochem J* 398 (2006) 107-112.
- [8] Y. de Keyzer, V. Valayannopoulos, J.F. Benoist, F. Batteux, F. Lacaille, L. Hubert, D. Chretien, B. Chadeveau-Vekemans, P. Niaudet, G. Touati, A. Munnich, P. de Lonlay, Multiple OXPHOS deficiency in the liver, kidney, heart, and skeletal muscle of patients with methylmalonic aciduria and propionic aciduria *Pediatr Res* 66 (2009) 91-95.

- [9] L. Gallego-Villar, C. Perez-Cerda, B. Perez, D. Abia, M. Ugarte, E. Richard, L.R. Desviat, Functional characterization of novel genotypes and cellular oxidative stress studies in propionic acidemia J Inherit Metab Dis 36 (2013) 731-740.
- [10] L. Gallego-Villar, A. Rivera-Barahona, C. Cuevas-Martin, A. Guenzel, B. Perez, M.A. Barry, M.P. Murphy, A. Logan, A. Gonzalez-Quintana, M.A. Martin, S. Medina, A. Gil-Izquierdo, J.M. Cuezva, E. Richard, L.R. Desviat, In vivo evidence of mitochondrial dysfunction and altered redox homeostasis in a genetic mouse model of propionic acidemia: Implications for the pathophysiology of this disorder Free Radic Biol Med 96 (2016) 1-12.
- [11] P. Wongkittichote, N. Ah Mew, K.A. Chapman, Propionyl-CoA carboxylase - A review Mol Genet Metab 122 (2017) 145-152.
- [12] L.R. Desviat, R. Sanchez-Alcudia, B. Perez, C. Perez-Cerda, R. Navarrete, R. Vijzelaar, M. Ugarte, High frequency of large genomic deletions in the PCCA gene causing propionic acidemia Mol Genet Metab 96 (2009) 171-176.
- [13] C. Perez-Cerda, B. Merinero, P. Rodriguez-Pombo, B. Perez, L.R. Desviat, S. Muro, E. Richard, M.J. Garcia, J. Gangoiti, P. Ruiz Sala, P. Sanz, P. Briones, A. Ribes, M. Martinez-Pardo, J. Campistol, M. Perez, R. Lama, M.L. Murga, T. Lema-Garrett, A. Verdu, M. Ugarte, Potential relationship between genotype and clinical outcome in propionic acidemia patients Eur J Hum Genet 8 (2000) 187-194.
- [14] J.P. Kraus, E. Spector, S. Venezia, P. Estes, P.W. Chiang, G. Creadon-Swindell, S. Mullerleile, L. de Silva, M. Barth, M. Walter, K. Walter, T. Meissner, M. Lindner, R. Ensenauer, R. Santer, O.A. Bodamer, M.R. Baumgartner, M. Brunner-Krainz, D. Karall, C. Haase, I. Knerr, T. Marquardt, J.B. Hennermann, R. Steinfeld, S. Beblo, H.G. Koch, V. Konstantopoulou, S. Scholl-Burgi, A. van Teeffelen-Heithoff, T. Suormala, M. Ugarte, W. Sperl, A. Superti-Furga, K.O. Schwab, S.C. Grunert, J.O. Sass, Mutation analysis in 54 propionic acidemia patients J Inherit Metab Dis 35 (2012) 51-63.
- [15] C.S. Huang, K. Sadre-Bazzaz, Y. Shen, B. Deng, Z.H. Zhou, L. Tong, Crystal structure of the alpha(6)beta(6) holoenzyme of propionyl-coenzyme A carboxylase Nature 466 (2010) 1001-1005.

- [16] L. Tong, Structure and function of biotin-dependent carboxylases Cellular and molecular life sciences : CMLS 70 (2013) 863-891.
- [17] B.L. Therrell, C.D. Padilla, J.G. Loeber, I. Kneisser, A. Saadallah, G.J. Borrajo, J. Adams, Current status of newborn screening worldwide: 2015 Semin Perinatol 39 (2015) 171-187.
- [18] E. Martinez-Morillo, B. Prieto Garcia, F.V. Alvarez Menendez, Challenges for Worldwide Harmonization of Newborn Screening Programs Clin Chem 62 (2016) 689-698.
- [19] J. Thusberg, A. Olatubosun, M. Vihinen, Performance of mutation pathogenicity prediction methods on missense variants Hum Mutat 32 (2011) 358-368.
- [20] S. Clavero, M.A. Martinez, B. Perez, C. Perez-Cerda, M. Ugarte, L.R. Desviat, Functional characterization of PCCA mutations causing propionic acidemia Biochim Biophys Acta 1588 (2002) 119-125.
- [21] C. Perez-Cerda, S. Clavero, B. Perez, P. Rodriguez-Pombo, L.R. Desviat, M. Ugarte, Functional analysis of PCCB mutations causing propionic acidemia based on expression studies in deficient human skin fibroblasts Biochim Biophys Acta 1638 (2003) 43-49.
- [22] T. Suormala, H. Wick, J.P. Bonjour, E.R. Baumgartner, Rapid differential diagnosis of carboxylase deficiencies and evaluation for biotin-responsiveness in a single blood sample Clin Chim Acta 145 (1985) 151-162.
- [23] I. Mochalkin, J.R. Miller, A. Evdokimov, S. Lightle, C. Yan, C.K. Stover, G.L. Waldrop, Structural evidence for substrate-induced synergism and half-sites reactivity in biotin carboxylase Protein Sci 17 (2008) 1706-1718.
- [24] M. Chloupkova, K.N. Maclean, A. Alkhateeb, J.P. Kraus, Propionic acidemia: analysis of mutant propionyl-CoA carboxylase enzymes expressed in Escherichia coli Hum Mutat 19 (2002) 629-640.
- [25] M. Chloupkova, K. Ravn, M. Schwartz, J.P. Kraus, Changes in the carboxyl terminus of the beta subunit of human propionyl-CoA carboxylase affect the oligomer assembly and catalysis: expression and characterization of seven patient-derived mutant forms of PCC in Escherichia coli Mol Genet Metab 71 (2000) 623-632.

- [26] H. Jiang, K.S. Rao, V.C. Yee, J.P. Kraus, Characterization of four variant forms of human propionyl-CoA carboxylase expressed in *Escherichia coli* J Biol Chem 280 (2005) 27719-27727.
- [27] N. Gregersen, P. Bross, S. Vang, J.H. Christensen, Protein misfolding and human disease Annu Rev Genomics Hum Genet 7 (2006) 103-124.
- [28] A.C. Muntau, J. Leandro, M. Staudigl, F. Mayer, S.W. Gersting, Innovative strategies to treat protein misfolding in inborn errors of metabolism: pharmacological chaperones and proteostasis regulators J Inherit Metab Dis 37 (2014) 505-523.
- [29] J. Underhaug, O. Aubi, A. Martinez, Phenylalanine hydroxylase misfolding and pharmacological chaperones Curr Top Med Chem 12 (2012) 2534-2545.
- [30] A. Gamez, P. Yuste-Checa, S. Brasil, A. Briso-Montiano, L.R. Desviat, M. Ugarte, C. Perez-Cerda, B. Perez, Protein misfolding diseases: Prospects of pharmacological treatment Clin Genet 93 (2018) 450-458.
- [31] R. Soemedi, K.J. Cygan, C.L. Rhine, J. Wang, C. Bulacan, J. Yang, P. Bayrak-Toydemir, J. McDonald, W.G. Fairbrother, Pathogenic variants that alter protein code often disrupt splicing Nat Genet 49 (2017) 848-855.
- [32] P. Forny, D.S. Froese, T. Suormala, W.W. Yue, M.R. Baumgartner, Functional characterization and categorization of missense mutations that cause methylmalonyl-CoA mutase (MUT) deficiency Hum Mutat 35 (2014) 1449-1458.
- [33] A.L. Pey, F. Stricher, L. Serrano, A. Martinez, Predicted effects of missense mutations on native-state stability account for phenotypic outcome in phenylketonuria, a paradigm of misfolding diseases Am J Hum Genet 81 (2007) 1006-1024.

## Legends to figures

**Figure 1. Propionic acidemia mutations identified in *PCCA* and *PCCB* genes.** Schematic representation of the genomic structure of the *PCCA* (panel A) and *PCCB* (panel B) genes, showing the location of the mutations identified in this work. Biotin carboxylase domain (BC), biotin transfer domain (BT) and biotin-carboxyl carrier protein domain (BCCP) are shown in the *PCCA* gene. The BC domain (amino acids 62-509) contains an ATP-binding domain and catalyzes the ATP-dependent carboxylation of biotin, the PCC cofactor bound to BCCP. BT domain is crucial for interactions with the carboxyl-transferase domain (CT) in the  $\beta$ -subunits encoded by *PCCB* gene, responsible of carboxyl-group transfer from biotin to the alpha carbon of propionyl-CoA.

**Figure 2. Functional analysis of *PCCA* and *PCCB* variants.** Representative blots of *PCCA* (panel A) and *PCCB* (panel B) proteins from lysates of *PCCA* and *PCCB*-deficient fibroblast cell lines co-transfected with the mutant *PCCA* or *PCCB* and the respective *PCCA* or *PCCB* wild-type constructs. At least two experiments were performed for each mutant construct. Control lanes correspond to untransfected samples. In each blot, GAPDH was used as loading control. Data represent the percentage of mutant *PCCA* or *PCCB* protein compared to wild-type. PCC activity for each variant is also shown as a percentage of that obtained with the wild-type constructs, which was set to 100%. Mutations in red result in partial PCC activity and protein levels; mutations in blue exhibit medium-high protein levels but no PCC activity.

**Figure 3. Location of disease-causing mutations in the PCC  $\alpha$ -subunit.** Cartoon representation using Pymol software of the catalytic region of the  $\alpha$ -subunit (green) and  $\beta$ - $\beta$  subunits interface (magenta and blue). Protein residues affected by mutations and key interacting residues are shown in sticks with the following atom colours: carbon, yellow for the mutant residues and the same colour as protein chain for others; nitrogen, blue; oxygen, red; sulphur, orange. Magnesium and chloride are represented as spheres. *PCCA* variants A)

p.A106E, B) p. Y121C, C) p.G142V, D) p.G175D, E) p.R230C, F) p.S252R, G) p.R399W, H) p.V431G, I) p.G456V, J) p.L470R, K) p.C712S.

**Figure 4. Location of disease-causing mutations in the PCC  $\beta$ -subunit.**

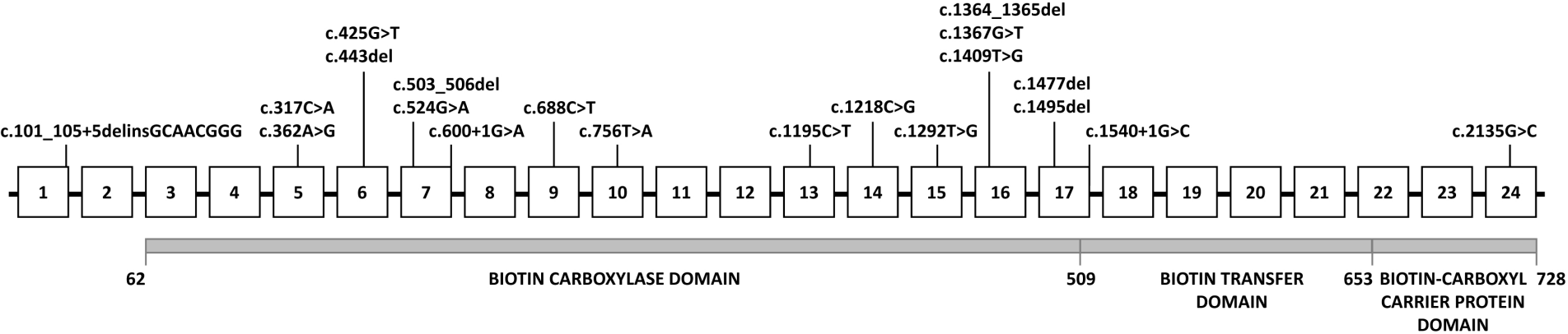
Cartoon representation using Pymol software of the catalytic region of the  $\alpha$ -subunit (green) and  $\beta$ - $\beta$  subunits interface (magenta and blue). Protein residues affected by mutations and key interacting residues are shown in sticks with the following atom colours: carbon, yellow for the mutant residues and the same colour as protein chain for others; nitrogen, blue; oxygen, red; sulphur, orange. Magnesium and chloride are represented as spheres. PCCB variants A) p.Q58P, B) p.E168del, C) p.G188A, D) p.H250Y, E) p.R272W, F) p.M316R, G) p.G356R, H) p.D382E, I) p.I460T, J) p.R512H, K) p.H534R.

**Figure 5. PCC activity and protein levels in patients' fibroblasts grown at different temperatures.**

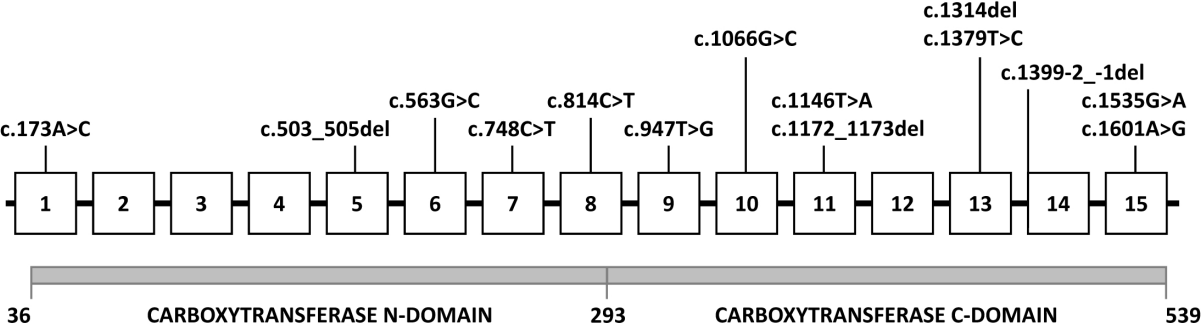
Control and patients (P8, P18 and P22) fibroblasts were grown at confluence at 28°C or at 37°C and PCC activity and protein levels analysed. Panel A shows the PCC activity relative to control levels at 37°C (mean 563.5 $\pm$ 96 pmol/min/mg). Data represent the mean $\pm$ standard deviation of at least 4 experiments. \* $p$ <0.05. Panels B and C show representative blots of PCCA and PCCB proteins, respectively, from lysates of control and patients' fibroblasts grown at each temperature. GAPDH was used as loading control. At least two experiments were performed.



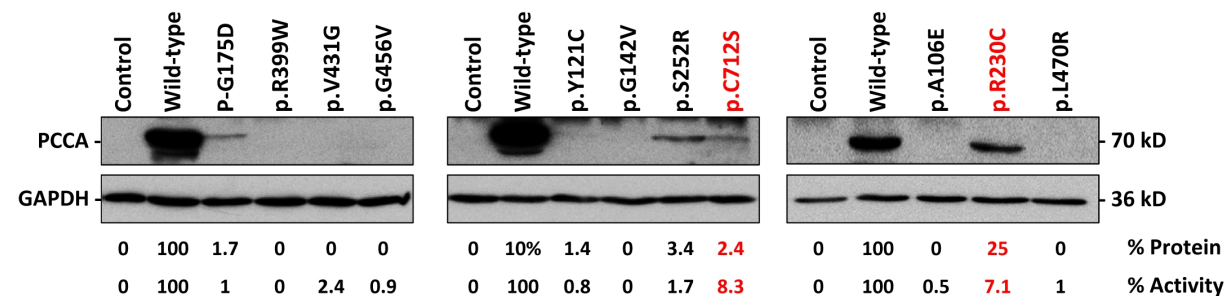
A) *PCCA*



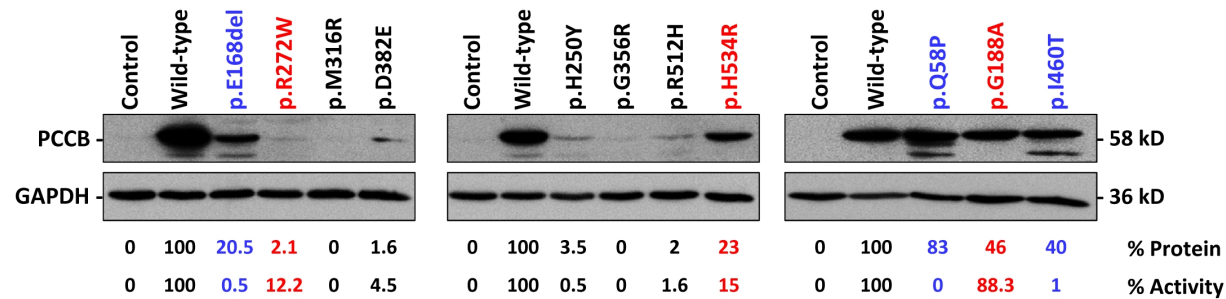
B) *PCCB*

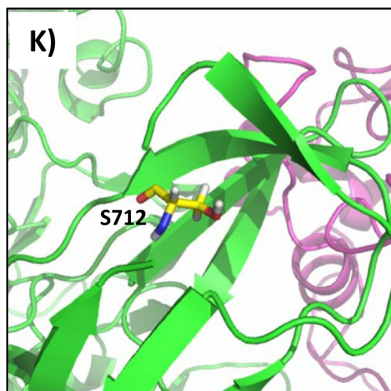
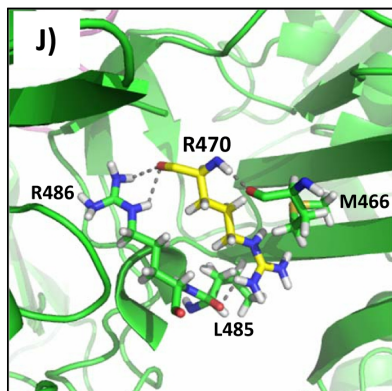
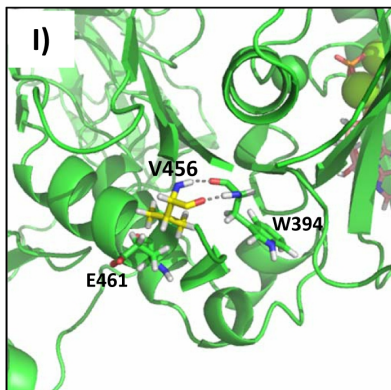
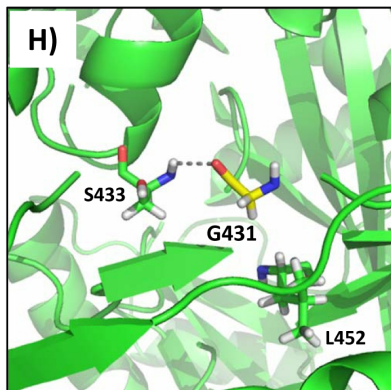
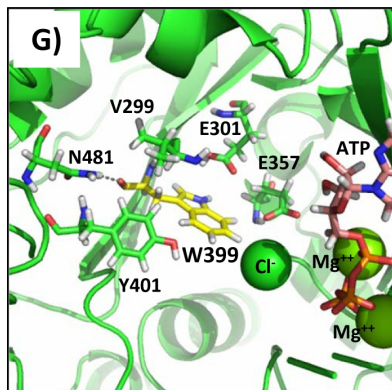
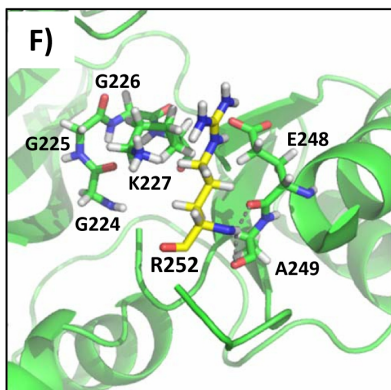
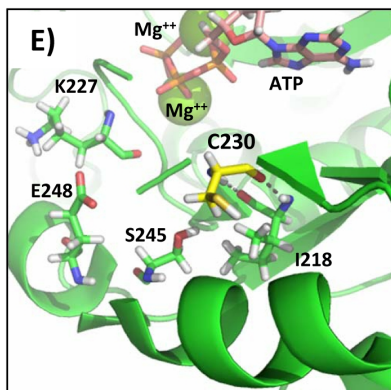
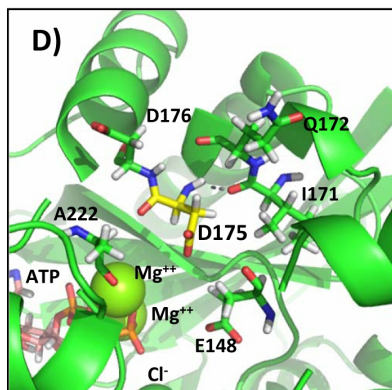
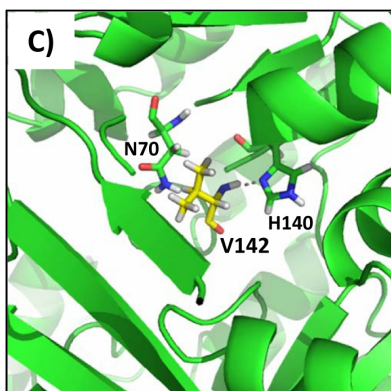
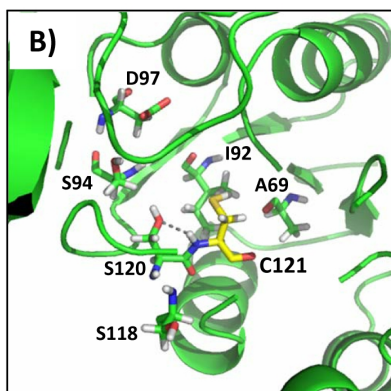
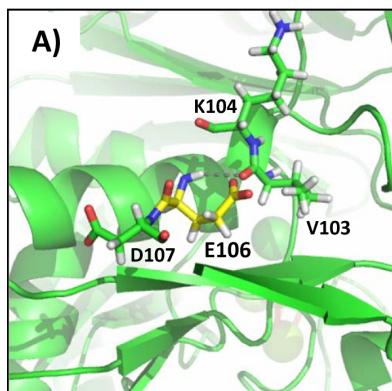


A) PCCA

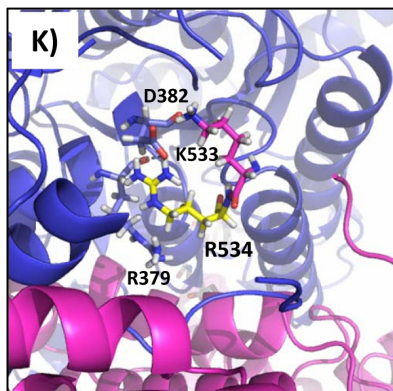
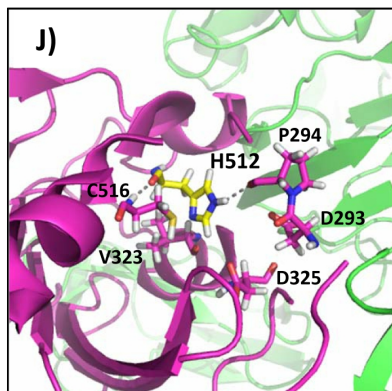
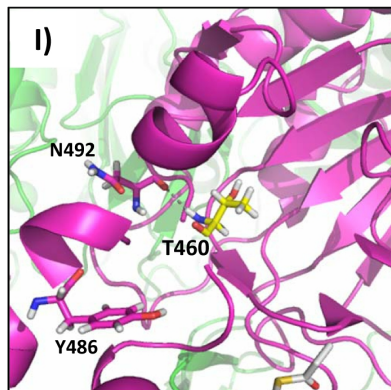
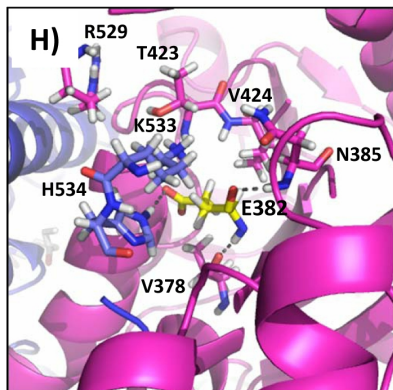
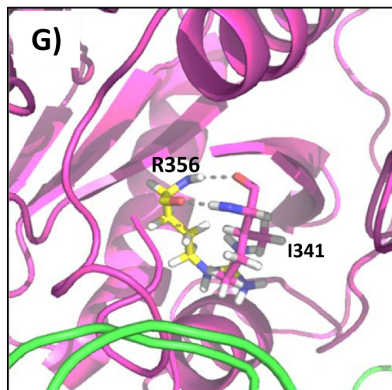
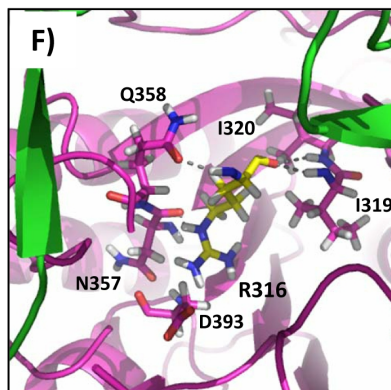
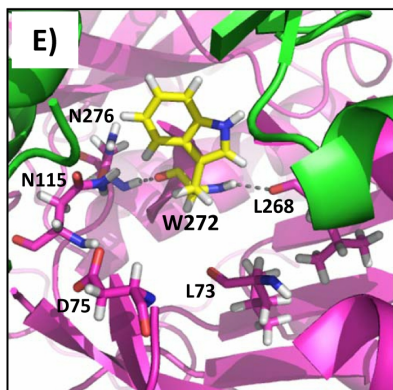
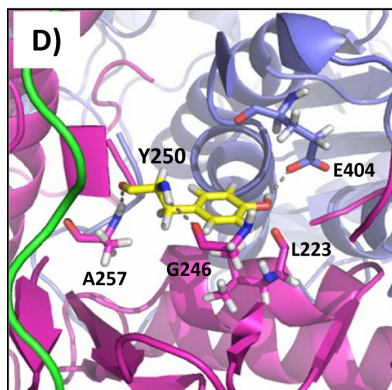
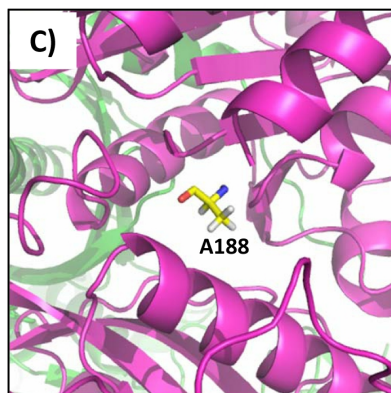
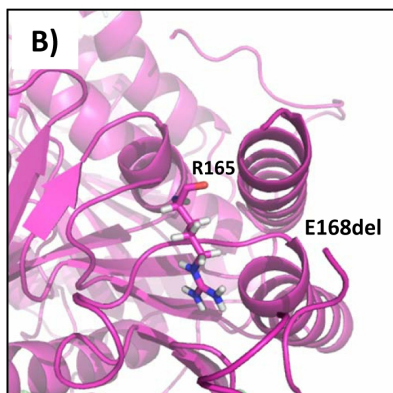
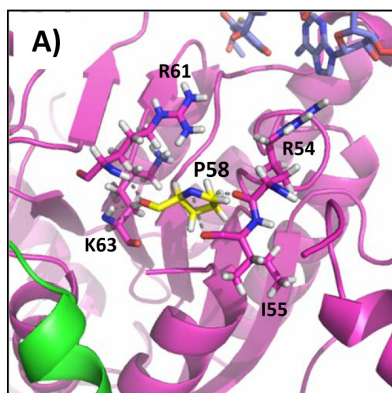


B) PCCB

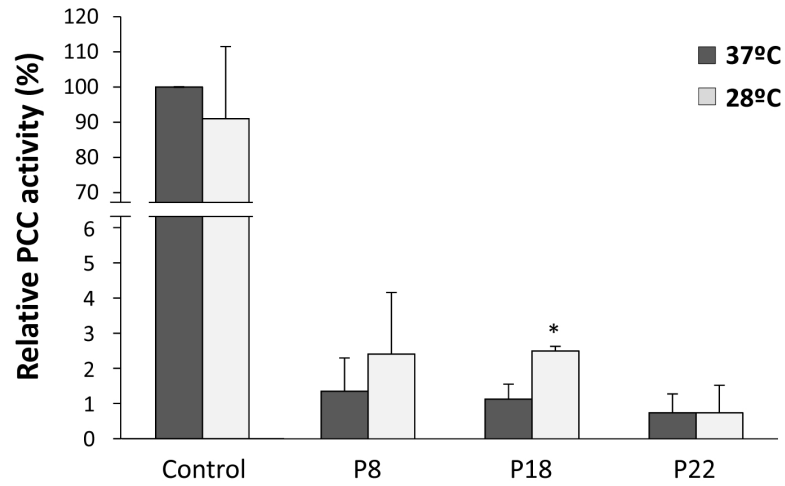




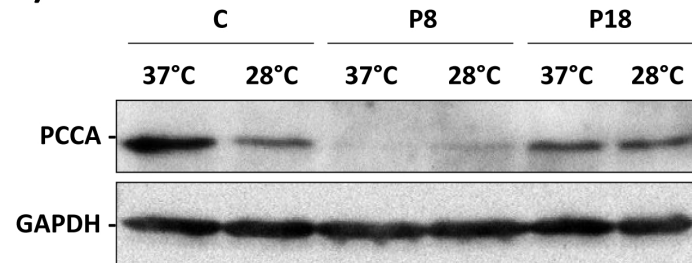




**A)**



**B)**



**C)**

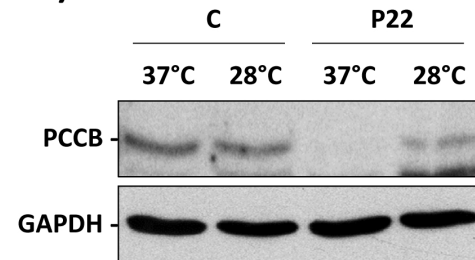


**Table 1. Genotype and available phenotypic data of PA patients with novel variants included in this study.**

| Deficient gene | Patient | Genotype <sup>1</sup>   | Presentation  | Available clinical notes   |
|----------------|---------|---|---------------|--|
| <b>PCCA</b>    | P1      | [c.101_105+5del10insGCAACGGG] + [c.101_105+5del10insGCAACGGG] | Neonatal      | Severe presentation, died at 10 days of age  |
|                | P2      | [c.317c>A] + [c.317c>A]                                       | Neonatal      | Severe presentation, hypotonia, taquipnea, metabolic acidosis  |
|                | P3      | [c.362A>G] + [c.362A>G]                                       | n.d.          | n.d.   |
|                | P4      | [c.425G>T] + [c.425G>T]                                       | n.d.          | n.d.   |
|                | P5      | [c.443delA] + [c.524G>A]                                      | Neonatal      | Severe presentation, several metabolic decompensations   |
|                | P6      | [c.503_506del] + [c.503_506del]                               | n.d.          | n.d.   |
|                | P7      | [c.600+1G>A] + [c.1367G>T]                                    | Neonatal      | n.d.   |
|                | P8      | [c.688C>T] + [c.184-618_300+3940]*                            | Late (2 yrs)  | Severe metabolic acidosis, lethargy, dehydrated upon admission to hospital   |
|                | P9      | [c.756T>A] + n.d.   | Early infancy | Severe presentation with encephalopathy and metabolic acidosis; currently adult with severe psychomotor delay            |
|                | P10     | [c.1195C>T] + [c.1195C>T]                                     | Neonatal      | Severe presentation  |
|                | P11     | [c.1218C>G] + [c.1292T>G]                                     | Neonatal      | Neurological deterioration, hypotonia  |
|                | P12     | [c.1540+1G>C] + [c.1364_1365del]                              | Neonatal      | Severe presentation, metabolic ketoacidosis. Alive at 7 yrs with psychomotor retardation.                                |
|                | P13     | [c.1409T>G] + [c.1409T>G]                                     | Neonatal      | Severe presentation, skin infection, anemia, hepatomegalia, hyperammonemia, neurological deterioration, severe hypotonia |
|                | P14     | [c.1409T>G] + [c.1409T>G]                                     | Neonatal      | Severe presentation, hypotonia, feeding difficulties   |
|                | P15     | [c.1409T>G] + [c.1409T>G]                                     | Neonatal      | Severe phenotype, frequent metabolic decompensations. Exitus at 4 yrs  |
|                | P16     | [c.1477delC] + [c.1831C>T]*                                   | -             | Prenatally diagnosed after previously affected sibling dead at 6 yrs of age  |
|                | P17     | [c.1495del] + [c.184-618_300+3940]*                           | NBS           | n.d.   |
|                | P18     | [c.2135G>C] + n.d.  | NBS           | n.d.   |

| Deficient gene | Patient | Genotype <sup>1</sup>                  | Presentation | Available clinical notes  |
|----------------|---------|--|--------------|---|
| <b>PCCB</b>    | P19     | [c.173A>C] + [c.1218_1231del13ins12]*  | n.d.         | Adult with mild clinical phenotype  |
|                | P20     | [c.503_505del] + [c.683C>T]*           | Late         | Cardiac and neurological complications, MELAS   |
|                | P21     | [c.563G>C] + [c.563G>C]                | Late         | Mild phenotype  |
|                | P22     | [c.748C>T] + [c.1218_1231del13ins12]*  | n.d.         | n.d. Alive at 6m  |
|                | P23     | [c.814C>T] + [c.737G>T]*               | Late (14 mo) | Convulsions with high temperature   |
|                | P24     | [c.947T>G] + [c.1146T>A]               | Neonatal     | Severe presentation with hypotonia and hyperammonemia at 48 h   |
|                | P25     | [c.1066G>C] + [c.1218_1231del13ins12]* | n.d.         | n.d.  |
|                | P26     | [c.1172_1173del] + [c.1172_1173del]    | Neonatal     | n.d.  |
|                | P27     | [c.1314del] + [c.1314del]              | n.d.         | n.d.  |
|                | P28     | [c.1379T>C] + [c.1399-2_-1del]         | NBS          | n.d.  |
|                | P29     | [c.1535G>A] + [c.493C>T]*              | NBS          | n.d.  |
|                | P30     | [c.1601A>G] + [c.1218_1231del13ins12]* | Neonatal     | Severe presentation, tachypnea, feeding refusal. Recurrent metabolic decompensations with convulsions. At 7 yrs of age, hypotonia, psychomotor and speech delay |

\*previously described mutation (HGMD Professional Release 2018.1). Mutation nomenclature has been updated according to HGVS (<http://varnomen.hgvs.org/>)

n.d. no data

NBS: newborn screening. yrs: years. mo:months

**Table 2. Missense mutations and in-frame deletions analysed in this work.**

| Gene        | Nucleotidic change | Aminoacidic change | Polyphen-2 (score) <sup>1</sup> | SIFT (score) <sup>2</sup> | MutPred (score) <sup>3</sup> | Mutation Taster <sup>4</sup> | Protein (%) | Activity (%) | Structural prediction     | Classification group <sup>5</sup> | Phenotype <sup>6</sup> |
|-------------|--------------------|--------------------|---------------------------------|---------------------------|------------------------------|------------------------------|-------------|--------------|---------------------------|-----------------------------------|------------------------|
| <b>PCCA</b> | c.317C>A           | p.A106E            | D (1.00)                        | D (0.00)                  | 0.881                        | D                            | 0           | 0.5          | Destabilizing             | 3                                 | Severe                 |
|             | c.362A>G           | p.Y121C            | D (1.00)                        | D (0.00)                  | 0.778                        | D                            | 1.4         | 0.8          | Destabilizing             | 3                                 | n.d.                   |
|             | c.425G>T           | p.G142V            | D (1.00)                        | D (0.00)                  | 0.971                        | D                            | 0           | 0            | Destabilizing             | 3                                 | n.d.                   |
|             | c.524G>A           | p.G175D            | D (0.98)                        | D (0.00)                  | 0.789                        | D                            | 1.7         | 1            | Distortion of active site | 2                                 | Severe                 |
|             | c.688C>T           | p.R230C            | D (1.00)                        | D (0.00)                  | 0.779                        | D                            | 25          | 7.1          | Destabilizing             | 1                                 | Late onset, moderate   |
|             | c.756T>A           | p.S252R            | D (0.97)                        | D (0.00)                  | 0.593                        | D                            | 3.4         | 1.7          | Destabilizing             | 3                                 | n.d.                   |
|             | c.1195C>T          | p.R399W            | D (1.00)                        | D (0.00)                  | 0.929                        | D                            | 0           | 0            | Distortion of active site | 2                                 | Severe                 |
|             | c.1292T>G          | p.V431G            | D (0.90)                        | D (0.01)                  | 0.806                        | D                            | 0           | 2.4          | Destabilizing             | 3                                 | Severe                 |
|             | c.1367G>T          | p.G456V            | D (1.00)                        | D (0.00)                  | 0.862                        | D                            | 0           | 0.9          | Destabilizing             | 3                                 | n.d.                   |
|             | c.1409T>G          | p.L470R            | D (1.00)                        | D (0.00)                  | 0.865                        | D                            | 0           | 1            | Destabilizing             | 3                                 | Severe                 |
|             | c.2135G>C          | p.C712S            | N (0.22)                        | D (0.30)                  | 0.747                        | D                            | 2.4         | 8.3          | Destabilizing             | 1                                 | n.d.                   |
| <b>PCCB</b> | c.173A>C           | p.Q58P             | D (1.00)                        | D (0.00)                  | 0.697                        | D                            | 83          | 0            | No substantial change     | 1/2                               | Mild                   |
|             | c.503_505del       | p.E168del          | -                               | -                         | -                            | D                            | 20.5        | 0.5          | Destabilizing             | 1/2                               | n.d.                   |
|             | c.563G>C           | p.G188A            | D (1.00)                        | D (0.00)                  | 0.814                        | D                            | 46          | 88.3         | No substantial change     | 1                                 | Mild                   |
|             | c.748C>T           | p.H250Y            | D (1.00)                        | D (0.00)                  | 0.836                        | D                            | 3.5         | 0.5          | Destabilizing             | 3                                 | n.d.                   |
|             | c.814C>T           | p.R272W            | D (1.00)                        | D (0.00)                  | 0.750                        | D                            | 2.1         | 12.2         | Destabilizing             | 1                                 | n.d.                   |
|             | c.947T>G           | p.M316R            | D (1.00)                        | D (0.00)                  | 0.858                        | D                            | 0           | 0            | Destabilizing             | 3                                 | Severe <sup>7</sup>    |
|             | c.1066G>C          | p.G356R            | N (0.12)                        | D (0.01)                  | 0.931                        | D                            | 0           | 0            | Destabilizing             | 3                                 | n.d.                   |
|             | c.1146T>A          | p.D382E            | D (0.98)                        | D (0.00)                  | 0.800                        | D                            | 1.6         | 4.5          | Destabilizing             | 3                                 | Severe <sup>7</sup>    |
|             | c.1379T>C          | p.I460T            | D (1.00)                        | D (0.00)                  | 0.855                        | D                            | 40          | 1            | Destabilizing             | 1/2                               | n.d.                   |
|             | c.1535G>A          | p.R512H            | D (1.00)                        | D (0.00)                  | 0.940                        | D                            | 2           | 1.6          | Destabilizing             | 3                                 | n.d.                   |
|             | c.1601A>G          | p.H534R            | D (1.00)                        | D (0.00)                  | 0.836                        | D                            | 23          | 15           | No substantial change     | 1                                 | Severe                 |

<sup>1</sup>PolyPhen-2: <http://genetics.bwh.harvard.edu/pph2/>. Score ranges from 0 (neutral, N) to 1 (damaging, D)

<sup>2</sup>SIFT: <http://sift.jcvi.org/>. Score ranges from 0 (damaging, D) to 1 (neutral, N)

<sup>3</sup>MutPred: <http://mutpred.mutdb.org/>. Scores >0.5 are predicted to be deleterious

<sup>4</sup>Mutation taster: <http://www.mutationtaster.org/>. D: disease causing

<sup>5</sup>group 1: destabilizing mutations with residual activity; group 2: catalytic mutations; group 3: destabilizing mutations with null or near-null activity

<sup>6</sup>In homozygous or functionally hemizygous patients; n.d. no data, there are no homozygous or functional hemizygous patients with that variant and/or no available clinical information

<sup>7</sup>Both mutations are in trans in P24



**Table 3. Structural analysis of point mutations in PCCA and PCCB proteins**

| Protein     | Amino acid change | Structural prediction; affected interactions between residues   |
|-------------|-------------------|---|
| <b>PCCA</b> | p.A106E           | Loss of hydrophobic interactions with nearby residues. Steric hindrance due to proximity to other negatively charged residues   |
|             | p.Y121C           | Loss of interaction with D97  |
|             | p.G142V           | Larger V142 residue narrows contact with I74, while keeping H-bond with H140. Possible repulsion with N70                       |
|             | p.G175D           | Change from a neutral residue to a hydrophilic one. Distortion of ATP, Mg <sup>++</sup> and Cl <sup>-</sup> binding site        |
|             | p.R230C           | Loss of salt bridge with E248. Prevents interaction with K227. Interactions between $\alpha$ -helix and $\beta$ -sheet affected |
|             | p.S252R           | New H-bond with E248. Steric hindrance due to repulsion with K227   |
|             | p.R399W           | Loss of interactions with E301, E357 and Y401. Disrupts ATP, Mg <sup>++</sup> and Cl <sup>-</sup> binding site                  |
|             | p.V431G           | G431 keeps interaction with S433. Loss of interaction with Val431 and Leu452  |
|             | p.G456V           | Possible interaction with Glu461  |
|             | p.L470R           | Distortion of hydrophobic core due to the introduction of a positive charge   |
|             | p.C712S           | No interactions affected  |
| <b>PCCB</b> | p.Q58P            | Distortion of $\alpha$ -helix at the beginning of polypeptide chain   |
|             | p.E168del         | Loss of interaction with R165. Localized in a loop between two $\alpha$ -helix  |
|             | p.G188A           | Located in a flexible region; no interactions affected  |
|             | p.H250Y           | New interaction with E404 in a different $\beta$ -chain. Possible loss of interaction with L223                                 |
|             | p.R272W           | Loss of interaction with L73, D75 and N115  |
|             | p.M316R           | Possible new interaction with D393 Introduction of a charged residue in a hydrophobic core                                      |
|             | p.G356R           | Steric hindrance due to proximity between R356 lateral chain and I341   |
|             | p.D382E           | Changes in the interactions between H534 and T423 from different $\beta$ -chains  |
|             | p.I460T           | T460 interacts with Y486 compensating for other interactions in hydrophobic pocket  |
|             | p.R512H           | Loss of H-bond with D293. Loss of interaction between D325 with V323 and P294   |
|             | p.H534R           | Loss of interaction with R379 and with K533, probably compensated by interaction with G421                                      |